This is an Accepted Manuscript version of the following article, accepted for publication in Journal of Hydraulic Research

Caterina Capponi, Aaron C. Zecchin, Marco Ferrante & Jinzhe Gong (2017): Numerical study on accuracy of frequency-domain modelling of transients, Journal of Hydraulic Research, 55(6), pp 813-828, DOI: 10.1080/00221686.2017.1335654.

It is deposited under the terms of the Creative Commons Attribution-NonCommercial-NoDerivatives License (http://creativecommons.org/licenses/by-nc-nd/4.0/), which permits non-commercial re-use, distribution, and reproduction in any medium, provided the original work is properly cited, and is not altered, transformed, or built upon in any way.

To appear in the *Journal of Hydraulic Research*
Vol. 00, No. 00, Month 20XX, 1–25

Research paper

Numerical study on accuracy improvement of linearized impulse-response modeling of transients in smooth pipes

CATERINA CAPPONI, PhD Student, *Dipartimento di Ingegneria Civile ed Ambientale, The University of Perugia, Via G. Duranti 93, 06125 Perugia, Italy*
Email: caterina.capponi@studenti.unipg.it (author for correspondence)

AARON C. ZECCHIN, Senior Lecturer, *School of Civil, Environmental and Mining Engineering, The University of Adelaide, South Australia 5005, Australia*
Email: aaron.zecchin@adelaide.edu.au

MARCO FERRANTE, Associate Professor, *Dipartimento di Ingegneria Civile ed Ambientale, The University of Perugia, Via G. Duranti 93, 06125 Perugia, Italy*
Email: marco.ferrante@unipg.it

JINZHE GONG, Research Associate, *School of Civil, Environmental and Mining Engineering, The University of Adelaide, South Australia 5005, Australia*
Email: jinzhe.gong@adelaide.edu.au

ABSTRACT
The integration of the governing equations of transients in the frequency domain has the appeal in that spatial discretization is not required, but the linearization of the equations is needed for the steady-friction term in turbulent flows. In this paper, to investigate the effects of such a linearization, a transient generated by a complete closure in a simple reservoir-pipe-valve system is considered, to exclude other linearization effects in the boundary conditions. A new approach is proposed to evaluate the linearized friction term, not only taking into account the flow dependency of the friction factor, but also changing the operating point where the friction term is evaluated. By means of this analysis significant improvements are gained in the frequency domain model performances for both elastic and viscoelastic pipes, in terms of their equivalence to the time domain models, which are not affected by the linearization error.

Keywords: Fluid transients, Frequency domain analysis, Time domain analysis, Viscoelasticity, Linear modeling, Steady-Friction, Linearization error

1 Introduction

Modeling pressure transients within pipeline systems has assumed a considerable importance in the last decades, since it allows the analysis of the pressure surge behavior in the system (Lee et al., 2013a; Zecchin et al., 2009) and to detect anomalies, like leaks (Brunone, 1999; Ferrante et al., 2009; Duan et al., 2010b; Gong et al., 2013, 2014; Zecchin et al., 2010), partial blockages (Lee et al., 2008; Meniconi et al., 2012b, 2013), illegal branches (Meniconi et al., 2011), and pipe wall deterioration (Stephens et al., 2013; Gong et al., 2015a).

When a transient is simulated, the governing equations (Wylie and Streeter, 1993; Chaudhry, 2014) can be solved in the time domain (e.g. with the Method of Characteristics, MOC), or, after being linearized, in the frequency domain. The main approaches used to model transients in the frequency domain for simple systems are the impedance method (IM) (Wylie, 1965) and the transfer matrix method (Chaudhry, 1970), while the impedance matrix method (Kim, 2007) and the admittance matrix method (Zecchin et al., 2009, 2010) are used to model more complex systems. Frequency-domain models can produce time-domain simulations by an inverse transform process, such as the inverse-Fourier transform (Ferrante and Brunone, 2003; Chaudhry, 1970; Suo and Wylie, 1989), or the inverse Laplace transform (Zecchin et al., 2012).

For a relatively simple system, the time domain modeling, by means of the MOC, is very accurate and provides a robust solution within a reasonable computational time, taking into account non-linearities such as friction. However, this model requires a fixed time-space grid that often implies approximations in the simulation of a transient, and, when the system becomes more complex, it takes a significant time for computation. The frequency domain models don't need a time-space grid so they can simulate precisely the arrival times of the reflected waves at a chosen measurement section (Suo and Wylie, 1989; Covas et al., 2005a). The solution of the Fourier transform of the linearized governing equations can be then evaluated in the time domain, so that these models map the system behavior from frequency to time and continuously in space. Moreover frequency domain models take less time for computation and are characterized by an easier code writing with respect to the MOC, especially when an increasingly complex system is considered (Zecchin et al., 2009, 2010). The efficiency of these models have been shown in a number of studies and applications (Ferrante and Brunone, 2003; Lee et al., 2006; Kim, 2007; Zecchin et al., 2011, 2013). Nevertheless, nonlinearities, like steady-friction, cannot be implemented in these models, as the use of the Fourier transform necessitates that the underlying equations be linear (Lee et al., 2005).

For the frequency-domain solution of the water hammer equations the transient signal is generally described as a perturbation about a mean state and then the Fourier transform is applied to the perturbed governing equations. Therefore, as outlined in detail in Wylie and Streeter (1993), the friction term is linearized about an operating point, that is the initial state of the system, so that the linearized term takes into account just the initial value of the flow in determining the linear resistance coefficient of the pipe. This, in case of a closure maneuver, can imply an overestimation of the friction term and therefore of the head losses, so that the damping of the pressure signal in the frequency domain models is faster than the true solution to the nonlinear equations. The linearization error of the frequency domain modeling with respect to the MOC have been investigated by Lee (2013) from an energy point of view and a comparison of the energy phase diagrams from the MOC and the frequency domain model has been provided for different transient events. Lee and Vìtkovsky (2010) have also quantified the linearization error occurring in frequency domain modeling due to the linearized steady-friction term and also to the linearization of the orifice equation, since the transients considered have been generated by a partial closure of the maneuver valve. When the closure is partial, the frequency domain model is expected to have a lower error with respect to the case of a complete closure, because the perturbation magnitude is smaller, as a percentage of the initial flow, and the part neglected in the linearization of the friction term is lower.

Viscoelasticity is an important effect that can be easily noticed when dealing with transients in polymeric pipes, such as polyvinyl chloride (PVC) and high density polyethylene (HDPE) pipes. When a viscoelastic pipe is considered, one of the most used ways to simulate the viscoelasticity is a generic Kelvin-Voigt model (Pezzinga et al., 2014). It can be implemented in both time and frequency domain models, without any linearization needed as the integro-differential operator that describes the viscoelastic effect is linear. The effects of the viscoelasticity have been studied and shown in both the domains by several authors (Gong et al., 2015b; Lee et al., 2013a; Duan et al., 2012; Covas et al., 2004, 2005b; Meniconi et al., 2012a). The viscoelastic effect produces a large attenuation of the transient signal, a significant smoothing, as well as a change in the oscillation period. It has been also shown that the viscoelasticity has a dominant effect with respect to the linearization error so that such error is less evident, giving place to a better reliability of the frequency domain model with respect to the elastic case.

This paper investigates the effect of the linearization of the friction term when transients are generated by a fast and complete closure of the downstream maneuver valve in a simple system (reservoir-pipe-valve), in both elastic and viscoelastic pipe cases. The fast complete closure increases the perturbation magnitude because it introduces the maximum disturbance that can be operated with respect to the mean state, so it can be considered the limiting worst case scenario for the frequency domain modeling: the higher such magnitude the higher the neglected term in the linearization. A non-linear boundary condition at the downstream end valve was not considered, as the focus of this work is to analyze the error due to the linearized friction term separately from other sources of error (e.g., a partial or a slow closure). The frequency domain model used in this analysis is based on the definition of the impedance and in the following is denoted as Impedance Methd model or IM (Ferrante and Brunone, 2003; Chaudhry, 1970; Suo and Wylie, 1989). In this paper is also introduced a linearization for the steady-friction term that takes into account the flow dependency of the friction factor, so that such linearization can be evaluated differently depending on the flow regime and the pipe relative roughness. In this work the attention has been focused on the smooth pipes. Furthermore, a correction factor is proposed to compensate the overestimation of the head losses and so to improve the performances of the frequency domain modeling. A strategy to find the best value for such correction factor is also presented, together with application examples that confirm the improvement in the equivalence between time and frequency domains model performance gained with this study.

2 Background

2.1 *The Impedance Method*

The 1-D water hammer continuity and momentum equations are (Wylie and Streeter, 1993; Chaudhry, 2014):

$$\frac{\partial H}{\partial t} + \frac{a^2}{gA}\frac{\partial Q}{\partial x} + k_{VE}(H) = 0 \tag{1}$$

$$\frac{\partial H}{\partial x} + \frac{1}{gA}\frac{\partial Q}{\partial t} + J(Q) = 0 \tag{2}$$

where H is the piezometric head, Q is the flow, x is the axial coordinate, t is the time, a is the wave speed, A is the pipe cross sectional area, g is the acceleration of gravity, k_{VE} is the viscoelasticity term and J is the term that takes into account the distributed head losses.

Eqs. (1) and (2) can be solved in time domain e.g. along a time-space grid with the MOC, or, after being linearized, they can be solved in the frequency domain by means of different methods. The approach outlined in Wylie and Streeter (1993) is presented here.

If the dependent variables in Eqs. (1) and (2) are considered as the sum of two components, e.g.

$H = \bar{H} + h'$ and $Q = \bar{Q} + q'$, so that the same equations hold for the mean values $\bar{H}$ and $\bar{Q}$, the equation in the perturbations h' and q' can be considered:

$$\frac{\partial h'}{\partial t} + \frac{a^2}{gA}\frac{\partial q'}{\partial x} + k_{VE}(h') = 0 \tag{3}$$

$$\frac{\partial h'}{\partial x} + \frac{1}{gA}\frac{\partial q'}{\partial t} + J'(q', \bar{Q}) = 0 \tag{4}$$

Taking the Fourier transform of Eqs. (3) and (4) yields:

$$i\omega h + \frac{a^2}{gA}\frac{\partial q}{\partial x} + k_{VE}(i\omega)h = 0 \tag{5}$$

$$\frac{\partial h}{\partial x} + \frac{i\omega}{gA}q + J'(i\omega, \bar{Q})q = 0 \tag{6}$$

where h and q are the Fourier transforms of the transient components h' and q', and $k_{VE}(i\omega)$ and $J'(i\omega, \bar{Q})$ are the Fourier transform of the operators $k_{VE}(\cdot)$ and $J'(\cdot, \bar{Q})$, respectively. The use of the impedance $Z(i\omega) = h(i\omega)/q(i\omega)$ allows analytic solutions of Eqs. (5) and (6) as shown in (Wylie, 1965) for a simple pipe system (R-P-V) or for more complex systems. The impedance , Z characterizes the resistance of the pipe during transients and its variation across each element of the system is described by upstream to downstream functions that relate transformed head and flow at different nodes (Suo and Wylie, 1989). As a consequence, the information pertaining the behavior of the system are contained all in one frequency dependent transfer function:

$$h(i\omega) = Z(i\omega)q(i\omega) \tag{7}$$

In time domain, the relationship between input and output signals is given by the convolutional integral:

$$h'(t) = \int_0^{+\infty} q'(\hat{t}) I(t - \hat{t}) d\hat{t} \tag{8}$$

where I is the impulse response function of the system (the inverse Fourier transform of the impedance Z) and contains the information about its behavior.

2.2 *Numerical system under consideration*

To assess the effect of the linearization error that occurs in frequency domain modeling, in this paper a reservoir-pipe-valve (R-P-V) system is considered and the IM results are compared to the MOC results. For different flow regimes the MOC solution is considered as a "true" solution, irrespective of MOC capabilities in representing the actual physical phenomenon, and this is the reason the differences between IM and MOC are also referred to as *errors*.

To reduce other errors due to the numerical integration and to henance the comparison, the discretization step of the MOC, Δt, is directly related to the discretization step in the frequency domain, $\Delta\omega$, with $\Delta t = (N\Delta\omega)^{-1}$. The used value of the the number of samples of the discretized signal, $N = 2^{20}$, allows to neglect the discretization errors (Lee et al., 2013b).

To give a more general character to this analysis, the following dimensionless quantities are used:

$$h^* = \frac{H - H_0}{\Delta H} \qquad ; \qquad t^* = \frac{t}{T} \tag{9}$$

where H is the piezometric head at the measurement section (i.e. immediately upstream the valve), H_0 is the initial value of H and has been fixed at the same value for all the simulations, ΔH is the Allievi-Joukowsky overpressure and T is the characteristic time of the pipe, respectively evaluated as:

$$\Delta H = \frac{a}{g}\frac{Q_0}{A} \qquad ; \qquad T = \frac{2L}{a} \tag{10}$$

with L being the length of the pipe, and Q_0 is the initial value of the flow.

The steady-friction term of Eq. (2) is evaluated as:

$$J = f(Q)\frac{|Q|Q}{2gDA^2} \tag{11}$$

where D is the pipe diameter and f is the Darcy-Weisbach friction factor and is evaluated with different formulas. For laminar flows, $J(Q)$ is linear and hence the time and frequency domain models coincide. For turbulent flows, $f(Q)$ can depend on the relative roughness of the pipe and the flow regime, i.e. the Reynolds number, Re. As highlighted in the introduction, the MOC is able to update at each point of the time-space grid the values of the flow, Q and so of J. Since the IM is not able to do this, it needs to linearize the friction term about an operating point, that is usually the initial state.

When the perturbation q' around the mean value $\bar{Q} \gg q'$ is introduced, the term $|\bar{Q}+q'|(\bar{Q}+q')$ can be rewritten as $(\bar{Q}+q')^2$ and J can be expanded by means of a Taylor series:

$$J(\bar{Q}+q') = J(\bar{Q}) + \frac{\dot{J}(\bar{Q})}{1!}q' + \frac{\ddot{J}(\bar{Q})}{2!}q'^2 + ... \tag{12}$$

where the number of dots over the letter indicates the order of the derivative with respect to Q.

Within the conventional IM, the linearization of J is operated considering f constant and equal to its initial value $f_0 = f(Q_0)$, so that the conventional linearized friction term for turbulent flows, hereafter referred as R_1, is:

$$R_1 = \frac{f_0\bar{Q}}{gDA^2} \tag{13}$$

In Fig. 1 the MOC result is shown for the R-P-V system in comparison with different IM approaches to show the IM performance affected by the linearization error. For the sake of clarity, in Fig. 1 are shown simulations in the case of elastic pipes, i.e. the viscoelasticity term, k_{VE}, in Eq. (1) is zero. The approach analyzed in this section, i.e. the IM using R_1, produces an unsatisfactory performance, since the differences with respect to the MOC solution are high. In the left side it can be observed that the linearization error causes differences between the two models that evolve with time, producing a different damping than the MOC. Within a short period analysis the error of the IM is small, but when an increasingly duration is considered, the differences with respect to the MOC increase. The remainder of this paper will investigate the linearization error, and present strategies to determine the optimal linear model to minimize this error.

3 Proposed linear approximation

In this section two approaches for determining linear resistance functions are introduced, aiming to improve the equivalence of the linearized model to the MOC. Firstly, a different linearization for the steady-friction term is proposed, considering the flow dependency of the friction factor. Secondly a correction factor is introduced to change the operating point where the friction term is linearized, in order to gain a better performance. Within this section, the proposed improvement strategies are outlined. Within the following section, these strategies are explored with a detailed computational strategy.

3.1 *Linearization of the steady-friction term including the friction factor derivative*

In order to introduce a more accurate linearized steady-friction term, from an analytical and a physical point of view, in this paper the linearization is derived considering that the friction factor, f, depends on Q and is not constant during the transient event.

Therefore, the series of Eq. (12) is the product of the two Taylor series, one for the friction factor, and one for the velocity head term:

$$J(\bar{Q}+q') = \left[f(\bar{Q}) + \frac{\dot{f}(\bar{Q})}{1!}q' + \frac{\ddot{f}(\bar{Q})}{2!}q'^2 + ...\right]\left[\frac{\bar{Q}^2}{2gDA^2} + \frac{2\bar{Q}}{2gDA^2}q' + \frac{1}{2gDA^2}q'^2 + ...\right] \tag{14}$$

By multiplying the terms, Eq. (14) becomes:

$$J(\bar{Q}+q') = f(\bar{Q})\frac{\bar{Q}^2}{2gDA^2} + \left[f(\bar{Q})\frac{2\bar{Q}}{2gDA^2} + \frac{\dot{f}(\bar{Q})}{1!}\frac{\bar{Q}^2}{2gDA^2}\right]q' + ... \tag{15}$$

Considering that the first term on the right hand is constant and it relates to the steady-state frictional losses that have been removed from the perturbation equations, and neglecting the terms of order ≥ 2 in the perturbation, the general form of the linearized steady-friction term, R', is given by the sum of the two terms in the brackets:

$$R' = f(\bar{Q})\frac{2\bar{Q}}{2gDA^2} + \dot{f}(\bar{Q})\frac{\bar{Q}^2}{2gDA^2} \tag{16}$$

For fully turbulent flow, since f does not depend on flow, $\dot{f}(Q) = 0$ and again $R' = R_1$ if $\bar{Q} = Q_0$. In general, it can be noted that, if f is considered constant, as in the conventional use of the IM, the second term in Eq. (16) becomes zero and R_1 is obtained. In the method presented in this paper, such term is no longer neglected and the proposed linearized steady-friction term is given by the sum of the two terms.

The evaluation of the linearized friction term depends on the formula used for f. In this paper the attention has been focused on the category of the smooth pipes in the case of turbulent flow, for which f is evaluated by means of the Blasius formula:

$$f(Q) = 0.316Re^{-0.25} = 0.316\left(\frac{QD}{\nu A}\right)^{-0.25} \tag{17}$$

where ν is the kinematic viscosity. Substituting Eq. (17) in Eq. (16), the proposed linearized friction term, R_2 is obtained:

$$\begin{aligned} R_2 &= 0.316\left(\frac{\bar{Q}D}{\nu A}\right)^{-0.25}\frac{2\bar{Q}}{2gDA^2} + 0.316\left(\frac{D}{\nu A}\right)^{-0.25}\left(-0.25\bar{Q}^{-1.25}\right)\frac{\bar{Q}^2}{2gDA^2} = \\ &= 0.316\left(\frac{D}{\nu A}\right)^{-0.25}\frac{1}{2gDA^2}1.75\bar{Q}^{0.75} = \qquad (18) \\ &= 0.875f(\bar{Q})\frac{\bar{Q}}{gDA^2} = 0.875R_1 \qquad (19) \end{aligned}$$

From an analytical point of view, the evaluation of R_2 is more correct since it considers the perturbation of the flow also within f and it does not neglect the second term of Eq. (16), while from a physical point of view, R_2 carries a coefficient that decreases the overestimation of the head losses with respect to R_1. It is worth of noting that such coefficient is less than 1, when the second term of Eq. (16) is no longer neglected. In Fig. 1 it is possible to observe that the signal simulated with the IM using R_2 presents a better performance than the one simulated using R_1 because the head losses are less overestimated, the damping is slower and so the differences with respect to the MOC are lower.

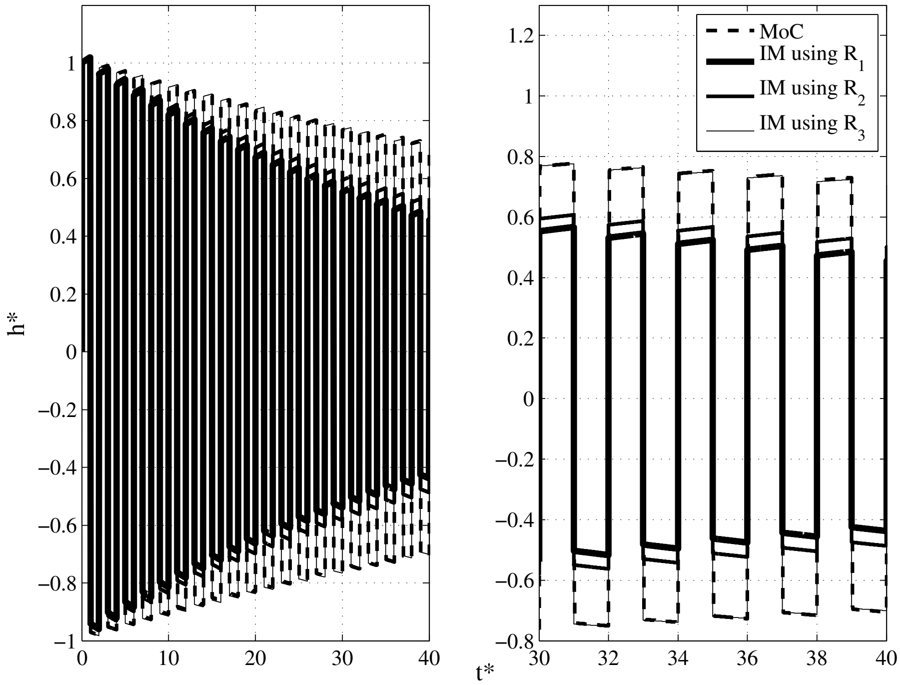

Figure 1 Dimensionless pressure signals obtained in a simple pipe system for $k_{VE} = 0$ by means of the MOC (dashed line) and three IM approaches (solid lines), using R_1, R_2 and R_3, where R_3 is evaluated with the correction factor $F = 0.5$. The MOC line and the IM line using R_3 are almost indistinguishable.

The improvement gained with the use of R_2 appears to be not enough to compensate the overestimation of the head losses with respect to the MOC. In fact, although a more equivalent form for the linearization has been developed, there is still a considerable overestimation of the head losses because the linearized friction term is still evaluated using the initial value of the flow $\bar{Q} = Q_0$ as the operating point.

3.2 *Correction factor*

Since during a transient generated by a full closure maneuver the flow at the valve varies from the initial value, Q_0, to 0, it can be presumed that a better improvement of the IM could be obtained using an average value of the flow to evaluate the linearized steady-friction term of Eq. (19). That is, the term J should in fact decrease with the flow, as maintaining it at a constant value based on the initial flow yields an overestimation of the frictional losses. Such average value is given by:

$$\bar{Q}(t) = C_{t^*} Q_0 \tag{20}$$

where $C \in [0, 1]$ is a coefficient that can assume different values depending on the duration of the simulation considered and that multiplies the initial value of the flow, Q_0. Introducing this expression in Eq. (19):

$$R_2 = C_{t^*}^{0.75} R_2|_{\bar{Q}=Q_0} \tag{21}$$

For simplicity, the correction factor $F = C_{t^*}^{0.75} \in [0, 1]$ is used hereafter to further decrease the effect of the linearization error. For the sake of clarity, the linearized friction term evaluated with F is referred as:

$$R_3 = F R_2 \tag{22}$$

In Fig. 1 a simulation carried out with the IM using R_3 with $F = 0.5$ is shown. It can be observed that the performance of this simulation is clearly better than the ones carried out using R_1 or R_2. Therefore, although it is not possible to update the value of the flow during the simulation, it is possible to evaluate a constant value of the friction term shifting the operating point by using not the initial value of the flow, that corresponds to $F = 1$, but a fraction of it. The issue of which is the optimal value of F to be used to gain the best performance in terms of the equivalence of the IM to MOC, depending on the transient conditions, is investigated in the next sections.

4 Numerical study of R_2

In order to have an indication of which range of F improves at best the performances of the IM, a numerical study is conducted for elastic and viscoelastic smooth pipes, considering that the optimal value (indicated with the superscript "*") of F depends on the flow regime, i.e. the initial Reynolds number, Re_0, and the duration of the simulation, t^*:

$$F^* = f(Re_0, t^*) \tag{23}$$

Signals are simulated for different values of Q_0 in order to have a set of tests within a range of Re_0 from 6.82 e03 to 1.36 e05. The flow regime, in fact, plays an important role in the assessment of the linearization error when a complete closure maneuver is operated, because the larger the Q_0, the larger the perturbation magnitude, the larger the error caused by the linearization of the steady-friction term. This is confirmed by Fig. 2 and Fig. 3, where simulations for elastic and viscoelastic pipes, respectively, are shown, comparing the MOC results with the signals carried out with the IM using R_2 (i.e. $F = 1$). So that, F^* is expected to be higher for the lowest values of Re_0 and lower as Re_0 increases. Comparing Fig. 2 and Fig. 3 the effect of viscoelasticity on the pressure signal and its effect on the analysis of the linearization error can be noted. The viscoelasticity term, k_{VE}, of Eq. (1) is represented by the linear Kelvin-Voigt (K-V) model (Pezzinga and Scandura, 1995) and is introduced in the frequency domain model as shown in Duan et al. (2012). The same ranges of Re_0 of the elastic case are used, but a shorter period is considered for the simulations, since the damping is faster when the viscoelasticity is introduced. It can be observed that the introduction of the viscoelasticity implies not only a faster damping and a smoothing effect, as already shown by Lee et al. (2013a), but also a reduction of the differences between the MOC and the IM signals. Viscoelasticity, in fact, for polymeric pipes, is a dominant effect with respect to the steady-friction and so the linearization error appears to be reduced, so that a better performance of the IM is expected in general. Nevertheless, in this paper, the introduction of the linearized friction term, R_3, is analyzed also for the viscoelastic pipes to improve the IM performance also in this case. Moreover, Duan et al. (2010a) have also shown that viscoelasticity is dominant with respect to unsteady friction when the quantity $P = (2DAa)/(fQ_0L)$ is greater than 1 (Ghidaoui et al., 2002). For the transients analyzed in this paper P ranges from a minimum of 17 to a maximum of

99 and so it allows to neglect the effect of the unsteady friction.

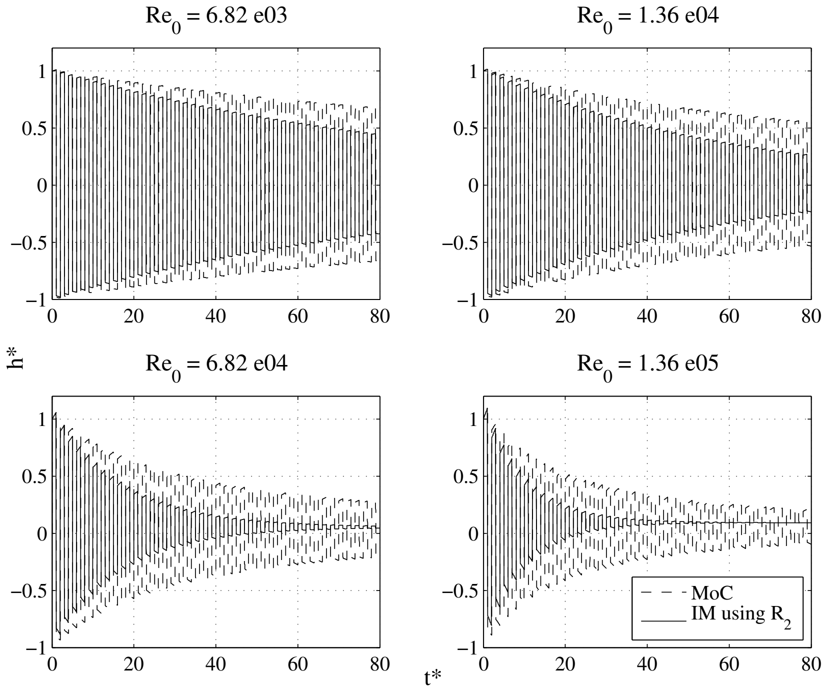

Figure 2 Comparison between dimensionless pressure signals obtained by means of the MOC and the IM approach using R_2 for 4 values of Re_0 in the case of elastic pipe.

The duration of the simulation influences the choice of F^* because the overestimation of the head losses evolves in time. So that, if only the first characteristic time lengths are considered, the linearization error is not so weighty and a relatively high F^* is expected. On the other hand, when an increasingly number of periods in considered, F^* has to compensate a higher overestimation of the head losses and so it is expected to be decreasing with the increase of the duration of the simulation.

When the differences between the IM and the MOC results are compared, the Nash-Sutcliffe coefficient, NS, is used as a goodness-of-fit index (Nash and Sutcliffe, 1970):

$$NS = 1 - \frac{\sum^n (h^*_{MOC} - h^*_{IM})^2}{\sum (h^*_{MOC} - \bar{h}^*_{MOC})^2} \tag{24}$$

in which h^*_{MOC} is the dimensionless pressure signal resulted from the MOC, $\bar{h}^*_{MOC}$ is its mean value, h^*_{IM} is the dimensionless pressure signal resulted from the IM, and n is the sample size. The NS coefficient can range from $-\infty$ to 1 and the closer the index is to 1, the more accurate the model is.

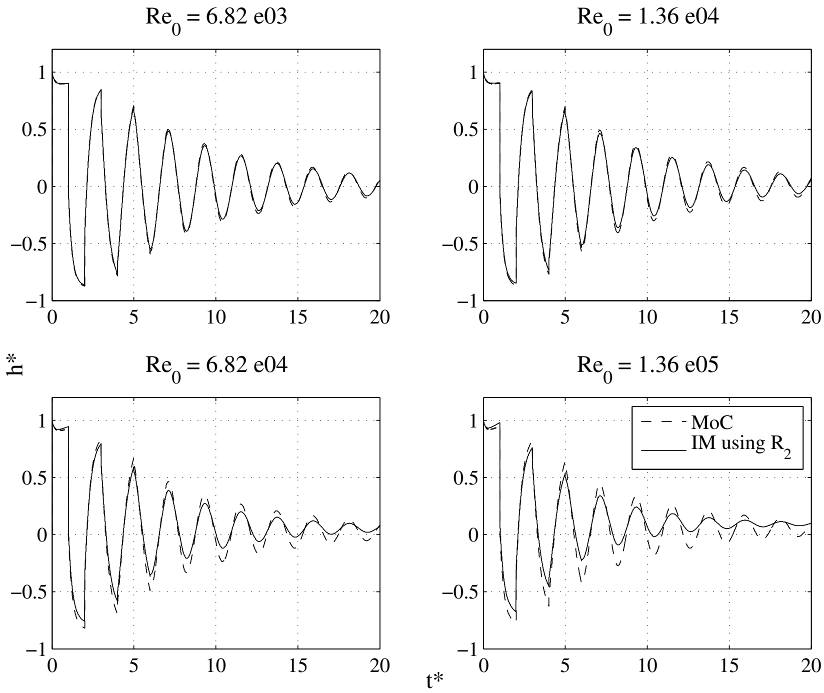

Figure 3 Comparison between dimensionless pressure signals obtained by means of the MOC and the IM approach using R_2 for 4 values of Re_0 in the case of viscoelastic pipe.

5 Optimal correction factor

5.1 *Parameter analysis: elastic pipes*

For different flow regimes (i.e. Re_0) and for different values of the duration, $t^* \in [0, 80]$, simulations are carried out using R_3, varying the value of the correction factor, F, and evaluating the NS coefficient to assess the goodness of the performance of the frequency domain model with respect to the MOC. In order to have a clear view of the trend of such performance, surface plots of NS (F, t^*) are given (Figs. 4 and 5). Since, the lighter the color of the surface, the higher the value of NS, it can be observed that for a short duration of the simulation ($t^* \simeq 4$), high values of NS are obtained for a large range of F, and this is true for all the flow regimes, so that F does not influences significantly the IM performance within approximately the first 4 characteristic times. When an increasing number of periods is considered, NS considerably decreases for the highest values of F, so it can be deduced that the conventional practice of using the 100 % of the linearized friction term (i.e. $F = 1$) will lead to a sub-optimal performance. This trend is more significant when Re_0 increases (Fig. 5).

To have a detailed view of the trend of NS when F is varied, slices of the 3D plots of Figs. 4 and 5 for $t^* = 4$, 20, 40 and 80 are given in Fig. 6. Such detailed view confirms that for $t^* = 4$ (Fig. 6a)

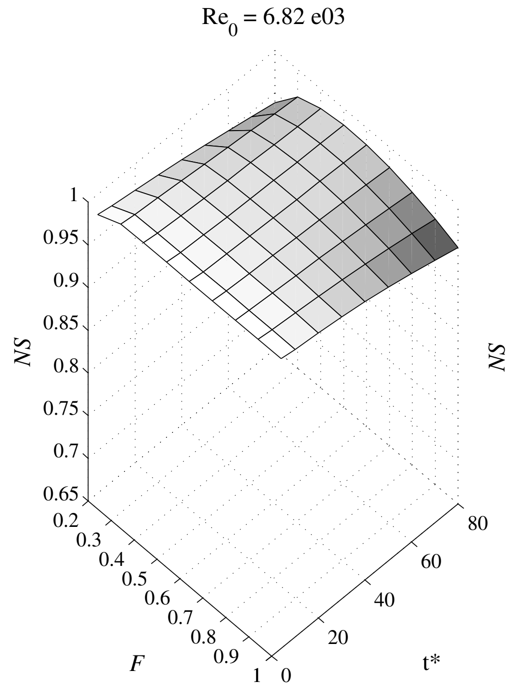

Figure 4 Surface plots for Re_0= 6.82 e03 and 1.36 e04, where NS is plotted against F and t^*, in the case of elastic pipe.

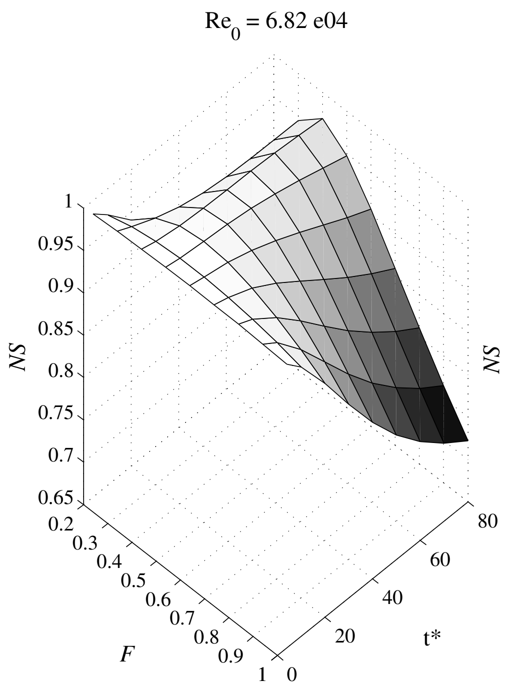

Figure 5 Surface plots for Re_0= 6.82 e04 and 1.36 e05, where NS is plotted against F and t^*, in the case of elastic pipe.

the influence of Re_0 is not significant, as each value of F provides a high NS. When an increasingly longer period is considered (Fig. 6b,c,d), it is more clear the effect of the overestimation of the head losses and the benefits gained using the correction factor. Particularly for the high values of Re_0, for which it is evident that the usual practice of taking into account the 100 % of the linearized friction term (i.e. $F = 1$) is disadvantageous, it is clear that a value of F between 0.4 and 0.6 provides a better performance. When the highest values of Re_0 are considered, the use of the correction factor becomes more important. In fact, if a higher value of F is used, the NS decreases dramatically and this is as true as it increases the period. For such values of Re_0 the optimal value of F is around 0.5, but it can decrease up to 0.4 if t^* becomes 40 or more. It can be also observed that even if a high value of Re_0 and t^* is considered, the optimal value of F is not smaller than 0.4.

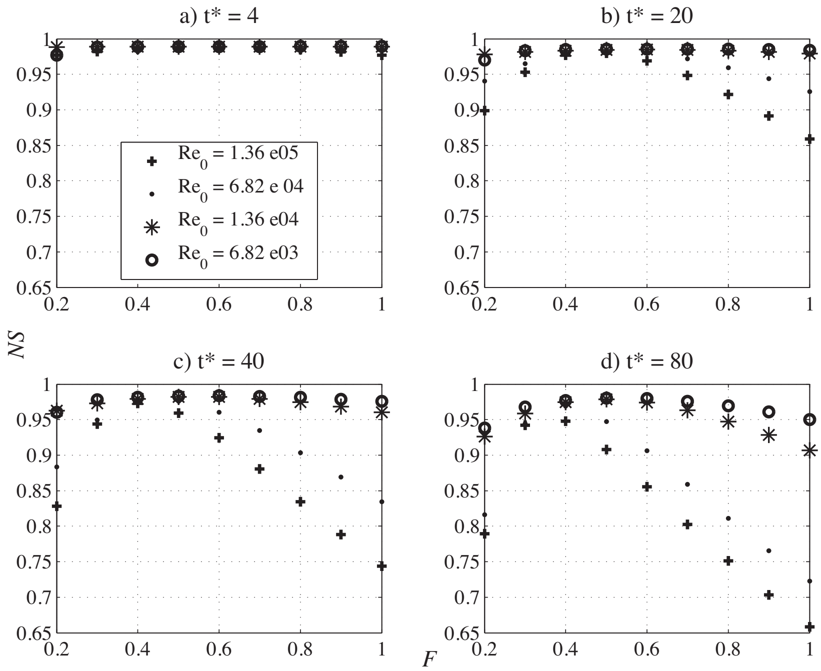

Figure 6 Variation of NS in function of F, for 4 values of Re_0 and for 4 values of t^*, for the case of elastic pipe.

To synthesize these observations in order to have a general indication of which is the optimal value of F to be used depending on the transient conditions, the diagram of Fig. 7 is shown. This figure shows which is the optimal value, F^*, to be used to obtain the highest NS depending on $t*$ and on the value of the initial Reynolds number. Therefore, when transients in elastic smooth pipes are modeled in the frequency domain, the linearized friction term, R_3, can be used. It can be evaluated using a value of F deduced from Fig. 7 that improves at best the model performance. This figure can be used as a “lookup” chart for F depending on the R-P-V system properties of interest.

To show the effects of this study in time domain, simulations for $t^* = 20$ and 80 using the found optimal values F^* are shown in Figs. 8, and 9. It is clear that the use of the optimal values of

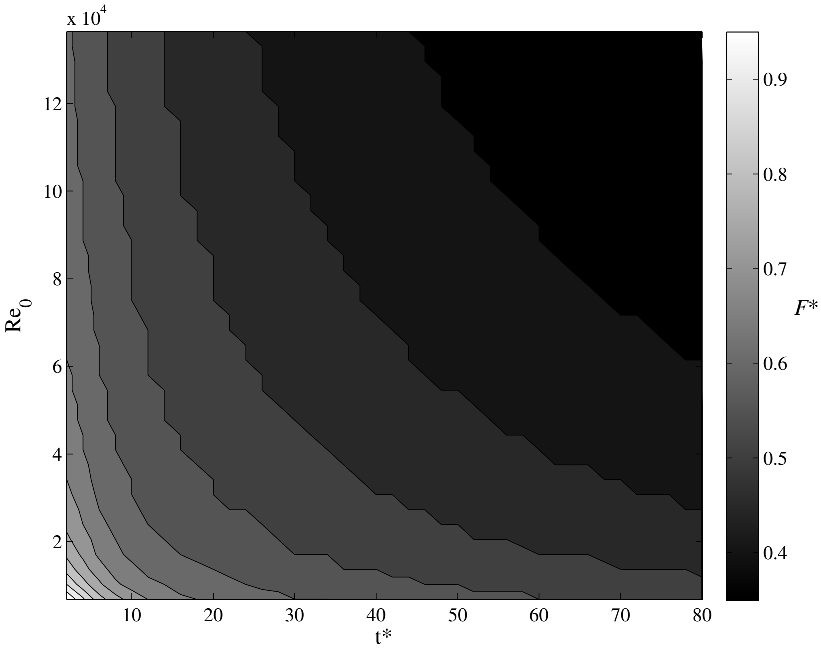

Figure 7 Diagram of the best values of the correction factor, F^*, to be chosen depending on Re_0 and t^* in order to have the maximum NS, for the case of elastic pipe.

F highly improves the IM performances and drastically reduce the linearization error occurring in frequency domain modeling. Comparing Fig. 9 with Fig. 2, that show the signals for the same duration ($t^* = 80$), it can be better noted that using the proposed linearized friction term, R_3, with the optimal value of F the IM provides a damping of the signal more similar to the one simulated with the MOC.

5.2 *Parameter analysis: viscoelastic pipes*

As in section 5.1, simulations are carried out using R_3, varying the value of the correction factor, F, and evaluating the NS coefficient for different flow regimes (i.e. Re_0) and for different values of the duration, $t^* \in [0, 40]$. Similarly to Figs. 4 and 5, the surfaces of Figs. 10 and 11 are obtained. Comparing the values of NS it can be noted that in general its values for the viscoelastic case are higher than the elastic one, as expected. For the lowest values of Re_0 (Fig. 10), NS has very high values and undergoes few changes, regardless of the value of the correction factor used, but from a numerical point of view it has been found that the optimal values of F for this flow conditions are around 0.65 for the shortest durations and can decrease to 0.35 for the longest ones. For the highest values of Re_0 considered (Fig. 11), the surfaces trend is very similar to Fig. 5, although NS varies in a narrower range and assumes higher values.

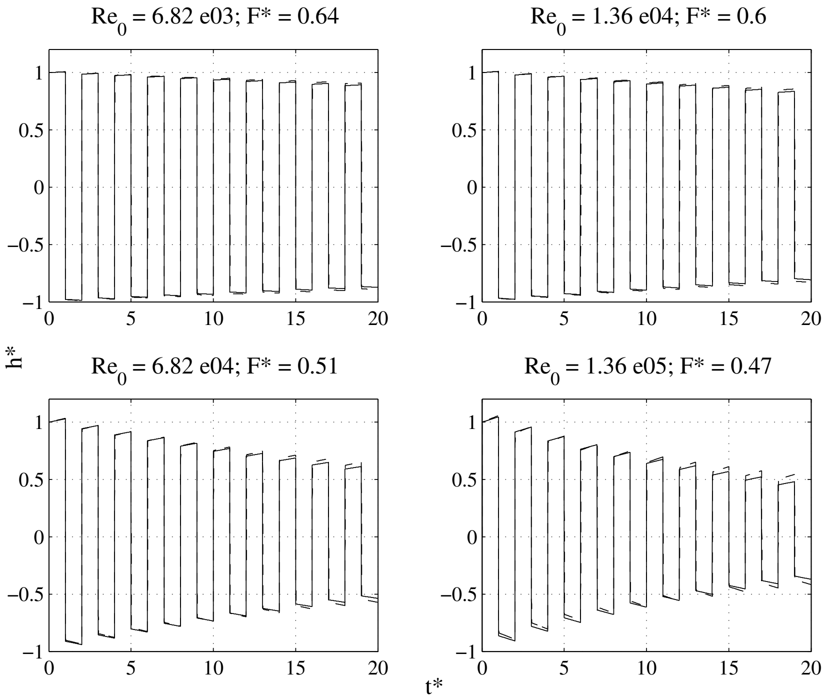

Figure 8 Comparison between dimensionless pressure signals for the case of elastic pipe, obtained by means of the MOC (dashed line) and by means of the IM approach using R_3 (solid line) with the best values F^* found in Fig. 7, for 4 values of Re_0 and for the duration $t^* = 20$.

At four values of t^* the surfaces of Figs. 10 and 11 are sliced in order to have a detailed view of the NS trend when F is varied (Fig. 12). Such trend is very similar to the elastic case (Fig. 6): the higher the Re_0 the more significant is the variation of NS with F.

To have a general indication of which is the optimal value F^* to be used depending on the transient conditions for the case of viscoelastic smooth pipes, the diagram of Fig. 13 is shown. Comparing this diagram with the one related to the elastic case (Fig. 7), it can be observed that the surface shape is different compared to the elastic case. In the viscoelastic case, in fact, the choice of the optimal F loses the strong dependance on Re_0, while the dependance on t^* is strengthened. From the color bar at the right side of Fig. 13 it can be observed that the F^* values are in the range 0.41 to 0.65, which is narrower than in the elastic case (0.38 to 0.98).

For one value of Re_0 and for two values of t^*, the optimal value F^* found with this analysis are used in the IM approach to carry out the two simulations for viscoelastic pipes that are presented in Fig. 14. Comparing these results with the simulation of Fig. 3 with $Re_0 = 6.82e04$, it can be noted that using the linearized friction term proposed in this paper, with the optimal value of F found by means of this analysis, a good improvement in the IM performance can be gained not only for the elastic pipes, but also for the viscoelastic ones. In fact, the value of NS increases when

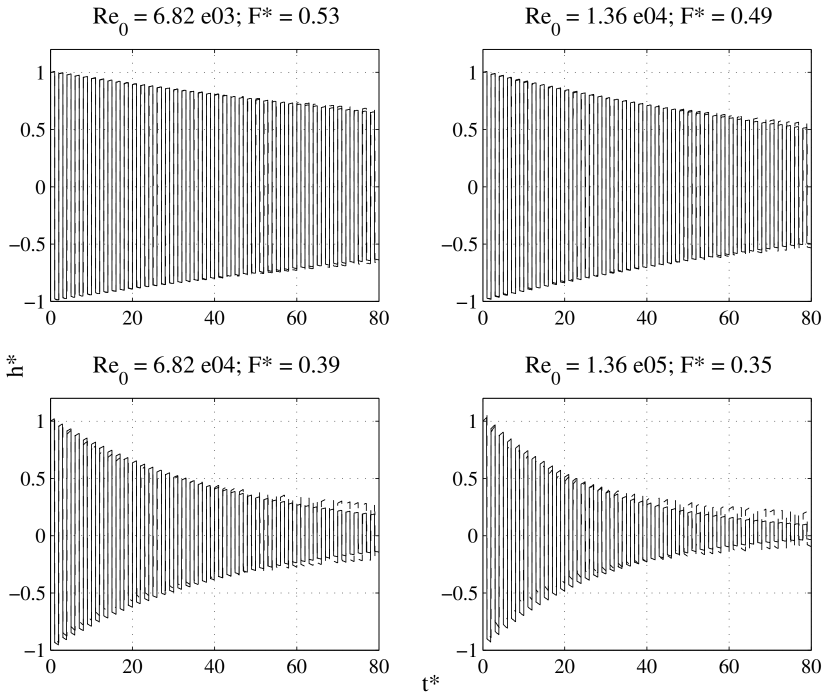

Figure 9 Comparison between dimensionless pressure signals for the case of elastic pipe, obtained by means of the MOC (dashed line) and by means of the IM approach using R_3 (solid line) with the best values F^* found in Fig. 7, for 4 values of Re_0 and for the duration $t^* = 80$.

the optimal F is used and the IM simulation is almost equivalent to the MOC one.

6 Conclusions

In this paper a R-P-V system subjected to transients generated by complete closure maneuvers has been considered in order to study the linearized steady-friction term separately from other sources of linearization error. Further studies are needed to study the linearization error effects in complex systems. Even if unsteady friction can be described using a linear model so that no linearization is needed in the frequency domain, for simplicity, it is not considered in this numerical study, but can be examined in further development of the method proposed in this paper. A more correct form for the linearized friction term has been proposed in order to involve the flow dependency of the friction factor in the linearization. Despite such new form, the linearization error has still produced a significant overestimation of the head losses during the transient event, because the operating point at which the linearized friction term is usually evaluated is the initial state, that corresponds to the maximum flow value that can be registered in transients generated by this type of maneuver. Given this, a correction factor has been introduced to change the operating point about which the linear resistance function is computed and so to use a fraction of the flow in the evaluation of

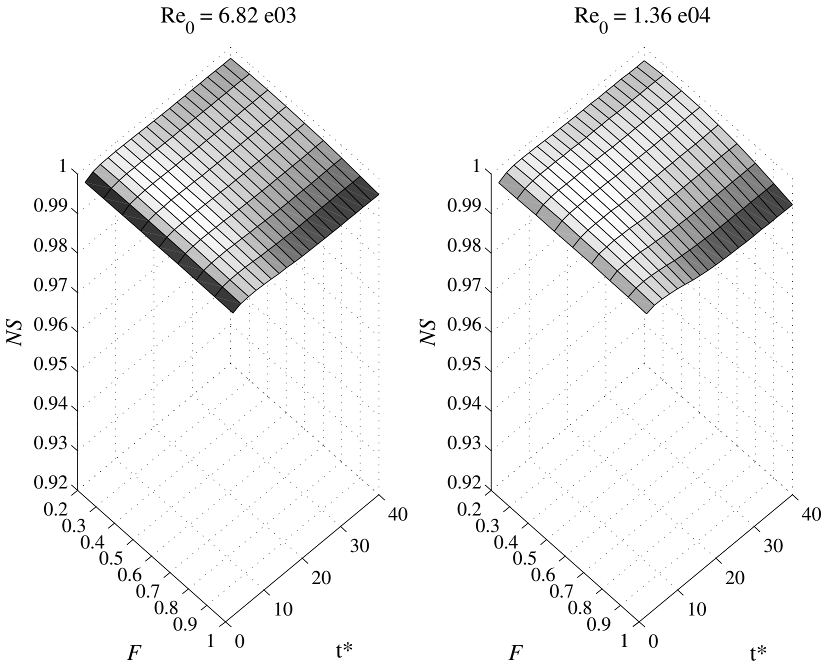

Figure 10 Surface plots for two low values of Re_0, where NS is plotted against F and t^*, in the case of viscoelastic pipe.

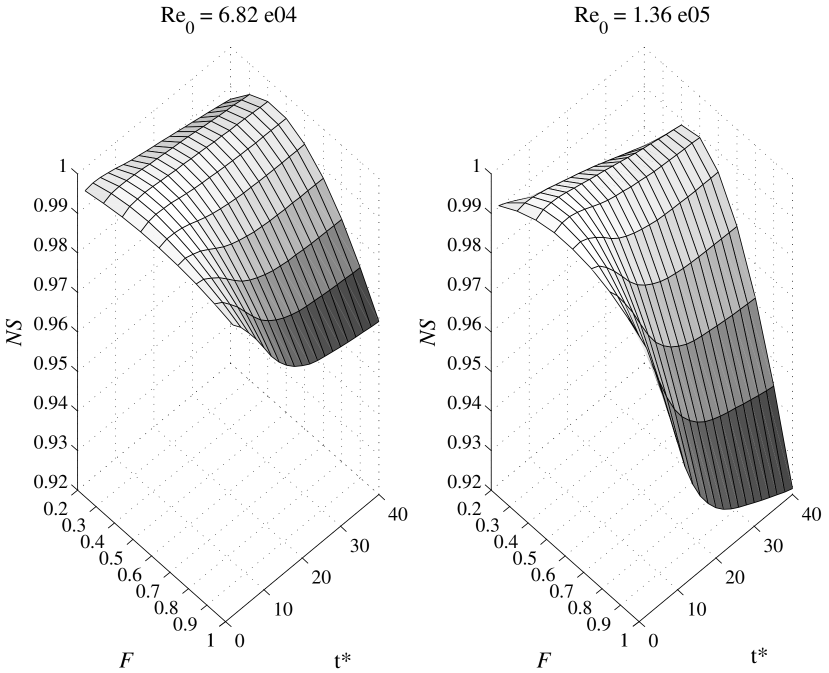

Figure 11 Surface plots for two high values of Re_0, where NS is plotted against F and t^*, in the case of viscoelastic pipe.

the linearized friction term to reduce the overestimation of the head losses with respect to the MOC results. Focusing the attention on the category of the smooth pipes, for both elastic and viscoelastic cases, and using the impedance method to present the frequency modeling results, a parameter analysis has been conducted to study the dependency of the correction factor on the

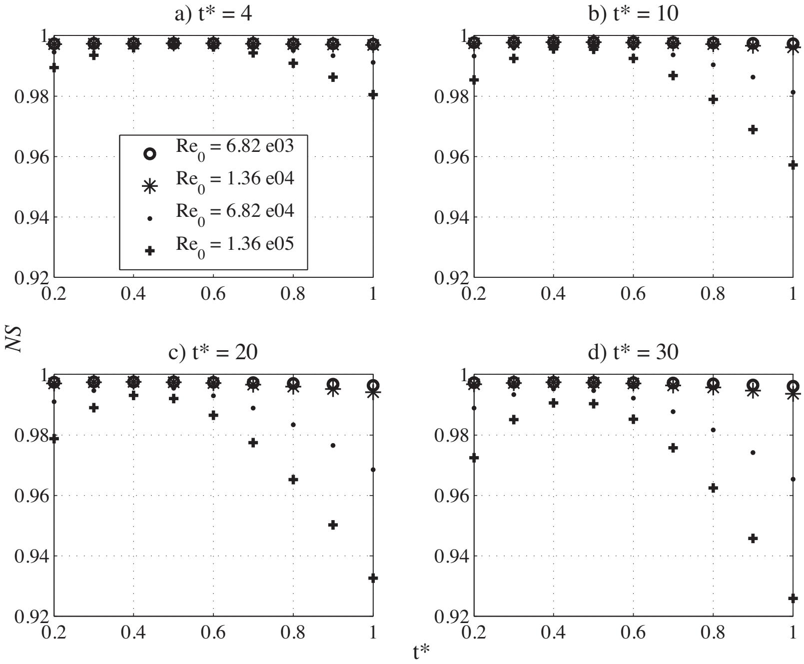

Figure 12 Variation of NS in function of F, for 4 values of Re_0 and for 4 values of t^*, for the case of viscoelastic pipe.

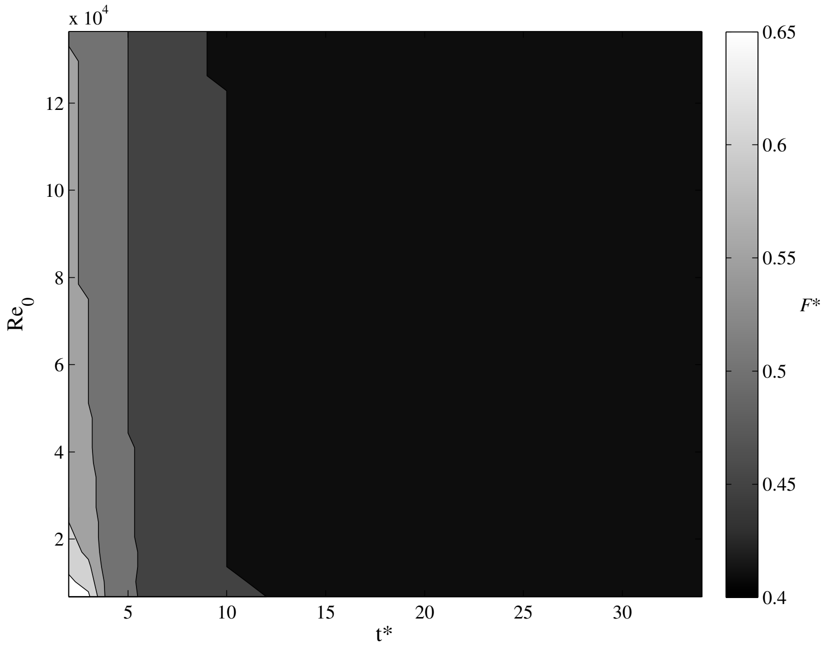

Figure 13 Diagram of the best values of the correction factor, F^*, to be chosen depending on Re_0 and t^* in order to have the maximum NS, for the case of viscoelastic pipe.

flow conditions and the duration of the simulation. Diagrams for elastic and viscoelastic cases have been produced to bring out the optimal values of the correction factor to be used depending on the system properties of interest. When the optimal value of F is used, the performance of the frequency domain modeling improves, in the sense that is almost equivalent to the MOC simulation,

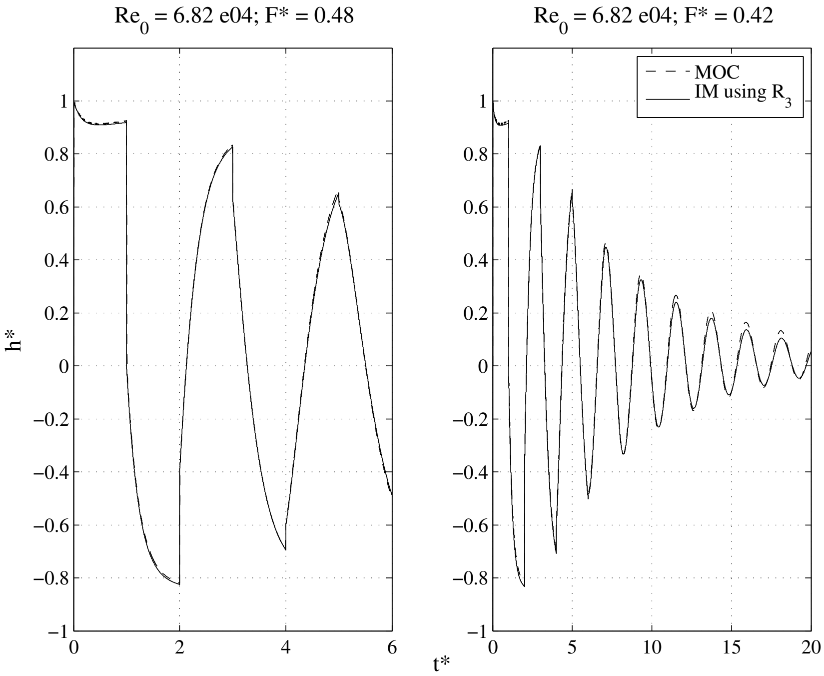

Figure 14 Comparison between dimensionless pressure signals for the case of elastic pipe, obtained by means of the MOC and by means of the IM approach using R_3 with the best values F^* found in Fig. 7, for 1 value of Re_0 and for the durations $t^* = 6$ (left side) and $t^* = 20$ (right side).

as shown in this paper for some transient conditions. These diagrams can be used in the practice as design charts to pick the optimal value for the correction factor in order to obtain a IM simulation as similar as possible to the MOC one.

Acknowledgments

This research has been funded by the University of Perugia and by the Italian Ministry of Education, University and Research (MIUR) under the Project of Relevant National Interest "Tools and procedures for an advanced and sustainable management of water distribution systems".

References

Brunone, B., 1999. Transient test-based technique for leak detection in outfall pipes. Journal of Water Resources Planning and Management 125, 302–306.

Chaudhry, M.H., 1970. Resonance in pressurized piping systems. J. Hydraul. Div., Am. Soc. Civ. Eng. 96, 1819–1839.

Chaudhry, M.H., 2014. Applied Hydraulic Transients. Springer New York.

Covas, D., Ramos, H., Almeida, A.B., 2005a. Impulse response method for solving hydraulic transients in viscoelastic pipes. XXXI IAHR Congress .

Covas, D., Stoianov, I., Mano, J.F., Ramos, H., Graham, N., Maksimovic, C., 2005b. The dynamic effect of pipe-wall viscoelasticity in hydraulic transients. Part II—model development, calibration and verification. Journal of Hydraulic Research 43, 56–70.

Covas, D., Stoianov, I., Ramos, H., Graham, N., 2004. The dynamic effect of pipe-wall viscoelasticity in hydraulic transients. Part I—Experimental analysis and creep characterization. Journal of Hydraulic Research 42, 517–532.

Duan, H.F., Ghidaoui, M., Lee, P.J., Tung, Y.K., 2010a. Unsteady friction and visco-elasticity in pipe fluid transients. Journal of Hydraulic Research 48, 354–362.

Duan, H.F., Lee, P.J., Ghidaoui, M.S., Tung, Y.K., 2010b. Essential system response information for transient-based leak detection methods. Journal of Hydraulic Research 48, 650–657.

Duan, H.F., Lee, P.J., Ghidaoui, M.S., Tung, Y.K., 2012. System Response Function-Based Leak Detection in Viscoelastic Pipelines. Journal of Hydraulic Engineering 138, 143–153.

Ferrante, M., Brunone, B., 2003. Pipe system diagnosis and leak detection by unsteady-state tests. 1. Harmonic analysis. Advances in Water Resources 26, 95–105.

Ferrante, M., Brunone, B., Meniconi, S., 2009. Leak-edge detection. Journal of Hydraulic Research 47, 233–241.

Ghidaoui, M.S., Mansour, S., Zhao, M., 2002. Applicability of quasisteady and axisymmetric turbulence models in water hammer. Journal of Hydraulic Engineering 128, 917–924.

Gong, J., Lambert, M.F., Simpson, A.R., Zecchin, A.C., 2013. Single-Event Leak Detection in Pipeline Using First Three Resonant Responses. Journal of Hydraulic Engineering 139, 645–655.

Gong, J., Stephens, M.L., Arbon, N.S., Zecchin, A.C., Lambert, M.F., Simpson, A.R., 2015a. On-site non-invasive condition assessment for cement mortar-lined metallic pipelines by time-domain fluid transient analysis. Structural Health Monitoring-an International Journal 14, 426–438.

Gong, J., Zecchin, A., Lambert, M., Simpson, A., 2015b. Study on the Frequency Response Function of Viscoelastic Pipelines Using a Multi-Element Kevin-Voigt Model. Procedia Engineering 119, 226–234.

Gong, J., Zecchin, A.C., Simpson, A.R., Lambert, M.F., 2014. Frequency Response Diagram for Pipeline Leak Detection: Comparing the Odd and Even Harmonics. Journal of Water Resources Planning and Management 140, 65–74.

Kim, S., 2007. Impedance matrix method for transient analysis of complicated pipe networks. Journal of Hydraulic Research 45, 818–828.

Lee, P.J., 2013. Energy analysis for the illustration of inaccuracies in the linear modelling of pipe fluid transients. Journal of Hydraulic Research 51, 133–144.

Lee, P.J., Duan, H.F., Ghidaoui, M., Karney, B., 2013a. Frequency domain analysis of pipe fluid transient behaviour. Journal of Hydraulic Research 51, 609–622.

Lee, P.J., Duan, H.F., Vitkovsky, J.P., Zecchin, A., Ghidaoui, M., 2013b. The effect of time–frequency discretization on the accuracy of the transmission line modelling of fluid transients. Journal of Hydraulic Research 51, 273–283.

Lee, P.J., Lambert, M.F., Simpson, A.R., Vitkovsky, J.P., 2006. Experimental verification of the frequency response method for pipeline leak detection. Journal of Hydraulic Research 44, 693–707.

Lee, P.J., Vìtkovsky, J.P., 2010. Quantifying Linearization Error When Modeling Fluid Pipeline Transients Using the Frequency Response Method. Journal of Hydraulic Engineering , 831–836.

Lee, P.J., Vítkovský, J.P., Lambert, M.F., 2005. Frequency domain analysis for detecting pipeline leaks. Journal of Hydraulic Engineering 131, 596–604.

Lee, P.J., Vitkovsky, J.P., Lambert, M.F., Simpson, A.R., Liggett, J.A., 2008. Discrete Blockage Detection in Pipelines Using the Frequency Response Diagram: Numerical Study. Journal of Hydraulic Engineering 134, 658–663.

Meniconi, S., Brunone, B., Ferrante, M., 2012a. Water-hammer pressure waves interaction at cross-section changes in series in viscoelastic pipes. Journal of Fluids and Structures 33, 44–58.

Meniconi, S., Brunone, B., Ferrante, M., Massari, C., 2011. Transient tests for locating and sizing illegal branches in pipe systems. Journal of Hydroinformatics 13, 334–345.

Meniconi, S., Brunone, B., Ferrante, M., Massari, C., 2012b. Transient hydrodynamics of in-line valves in viscoelastic pressurized pipes: long-period analysis. Experiments in fluids 53, 265–275.

Meniconi, S., Duan, H.F., Lee, P.J., Brunone, B., Ghidaoui, M.S., Ferrante, M., 2013. Experimental Investigation of Coupled Frequency and Time-Domain Transient Test-Based Techniques for Partial Blockage Detection in Pipelines. Journal of Hydraulic Engineering 139, 1033–1040.

Nash, J.E., Sutcliffe, J.V., 1970. River flow forecasting through conceptual models part I — A discussion of principles. Journal of Hydrology 10, 282–290.

Pezzinga, G., Brunone, B., Cannizzaro, D., Ferrante, M., Meniconi, S., Berni, A., 2014. Two-

Dimensional Features of Viscoelastic Models of Pipe Transients. Journal of Hydraulic Engineering 140, 04014036.

Pezzinga, G., Scandura, P., 1995. Unsteady-Flow in Installations with Polymeric Additional Pipe. Journal of Hydraulic Engineering-Asce 121, 802–811.

Stephens, M.L., Lambert, M.F., Simpson, A.R., 2013. Determining the Internal Wall Condition of a Water Pipeline in the Field Using an Inverse Transient. Journal of Hydraulic Engineering 139, 310–324.

Suo, L., Wylie, B.E., 1989. Impulse Response Method for Frequency-Dependent Pipeline Transients. Journal of Fluids Engineering 111, 478–483.

Wylie, B.E., 1965. Resonance in Pressurized Piping Systems. Journal of Basic Engineering 87, 960–966.

Wylie, B.E., Streeter, V.L., 1993. Fluid Transients in Systems. Prentice Hall, Englewood Cliffs, NJ, USA.

Zecchin, A.C., Lambert, M.F., Simpson, A.R., 2011. Inverse Laplace Transform for Transient-State Fluid Line Network Simulation. Journal of Engineering Mechanics 138, 101–115.

Zecchin, A.C., Lambert, M.F., Simpson, A.R., 2012. Inverse Laplace Transform for Transient-State Fluid Line Network Simulation. Journal of Engineering Mechanics 138, 101–115.

Zecchin, A.C., Lambert, M.F., Simpson, A.R., White, L.B., 2010. Frequency-Domain Modeling of Transients in Pipe Networks with Compound Nodes Using a Laplace-Domain Admittance Matrix. Journal of Hydraulic Engineering 136, 739–755.

Zecchin, A.C., Simpson, A.R., Lambert, M.F., White, L.B., Vitkovsky, J.P., 2009. Transient Modeling of Arbitrary Pipe Networks by a Laplace-Domain Admittance Matrix. Journal of Engineering Mechanics-Asce 135, 538–547.

Zecchin, A.C., White, L.B., Lambert, M.F., Simpson, A.R., 2013. Parameter identification of fluid line networks by frequency-domain maximum likelihood estimation. Mechanical Systems and Signal Processing 37, 370–387.